Enumeration of Messy Polygon Mosaics

Jack Hanke
Northwestern University

Michael Maltenfort
Northwestern University

Abstract

Hong and Oh introduced a model for multiple ring polymers in physics in which an $m \times n$ matrix is constructed from a selection of 7 distinct tiles. These matrices are called *mosaics*. The authors provide bounds on a subset of these mosaics that have the property of being suitably connected. These mosaics are called *polygon mosaics* because the tiles in a suitably connected mosaic form polygons. We introduce and enumerate mosaics with the related property of containing at least one polygon, which we call messy polygon mosaics.

1 Introduction

Hong and Oh [2] introduced a model for multiple ring polymers in which an $m \times n$ matrix is constructed using 7 distinct symbols callet *tiles*. These tiles, diagrammed in Figure 1, are composed of unit squares with dotted lines connecting 2 sides at their midpoint, as well as the "blank" tile T_0.

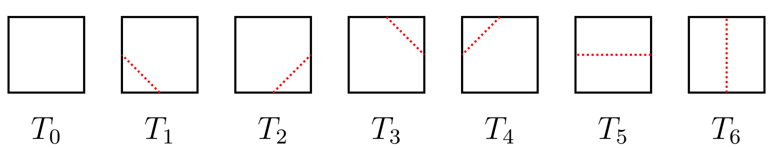

Figure 1: The tile set $\mathbb{T}$

We denote the set of tiles $\mathbb{T} = \{T_0, \ldots, T_6\}$. An (m, n) *mosaic* is an $m \times n$ matrix made up of elements from $\mathbb{T}$. Figure 2a shows a $(5, 7)$ mosaic. We denote the set of all (m, n) mosaics as $\mathbb{M}^{(m,n)}$. As there are 7 elements in $\mathbb{T}$, there are 7^{mn} mosaics in $\mathbb{M}^{(m,n)}$.

The authors in [2] were interested in mosaics with the property of being *suitably connected*, which is defined as follows. Consider an edge shared between two tiles in Figure 2a. The edge has either 0, 1, or 2 dotted lines drawn from its midpoint. Also note that the outer edges of the tiles on the boundary of the matrix are not shared by another tile. Therefore these edges only have 0 or 1 dotted lines drawn from their midpoint. A mosaic is suitably connected if all edges have 0 or 2 dotted lines drawn from their midpoint. The authors call mosaics that are suitably connected and that contain at least one tile in $\mathbb{T} \setminus T_0$ *polygon mosaics* because

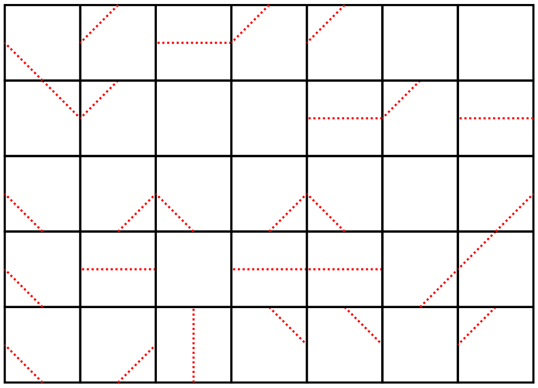

(a) A mosaic

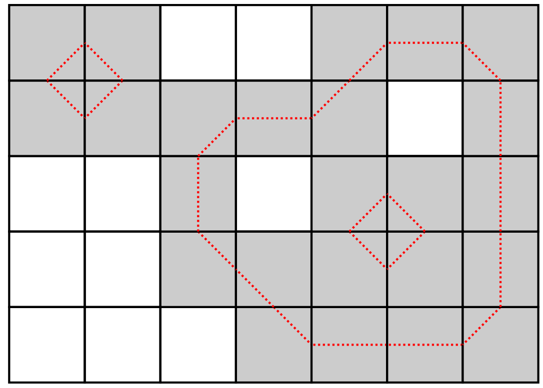

(b) A polygon mosaic

Figure 2: Examples of mosaics of size $(5, 7)$ made of tiles in $\mathbb{T}$

the dotted lines form *polygons*[1]. Following [2], when we use the term polygon in this work, we specifically refer to the set of tiles for which the dotted lines form a polygon when part of a mosaic.

Example 1.1. Figure 2b shows a polygon $(5, 7)$ mosaic that contains 3 polygons, with the tiles that make up the polygons shaded in gray. Note that a mosaic can contain polygons that surround other polygons, such as in Figure 2b.

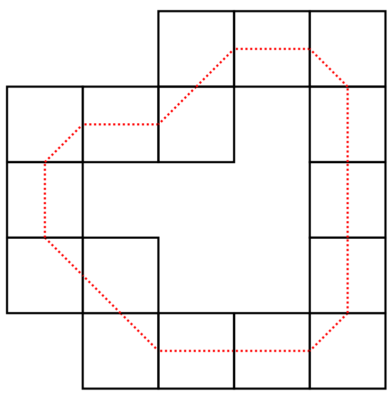

Figure 3: A polygon in Figure 2b

Using the notation conventions in [9], we denote the subset of (m, n) mosaics that are polygon mosaics as $\mathbb{P}^{(m,n)}$.

Theorem 1.1 ([2])**.** *The number of polygon (m, n) mosaics $|\mathbb{P}^{(m,n)}|$ for $m, n \geq 3$ is bounded by*

$$2^{m+n-3}\left(\frac{17}{10}\right)^{(m-2)(n-2)} \leq |\mathbb{P}^{(m,n)}| \leq 2^{m+n-3}\left(\frac{31}{16}\right)^{(m-2)(n-2)}.$$

[1]Polygons are more commonly refered to as "self-avoiding polygons" in the literature to highlight their connection with self-avoiding walks.

The array of values of $|\mathbb{P}^{(m,n)}| + 1$ is sequence A181245 on the OEIS [4, OEIS].

In related work, Lomonaco and Kauffman [3] introduced mosaics constructed from a tile set of 11 distinct tiles, of which $\mathbb{T}$ is a subset. The authors call mosaics constructed from this tile set that are suitably connected *knot mosaics*. Oh et al. [9] enumerated the number of knot mosaics.

Theorem 1.2 ([9]). *The number of knot mosaics of size (m,n) for $m,n \geq 2$ is $2\,\|(X_{m-2}+O_{m-2})^{n-2}\|$, where $X_0 = O_0 = \begin{bmatrix}1\end{bmatrix}$ and X_{m-2} and O_{m-2} are $2^{m-2} \times 2^{m-2}$ matrices defined as*

$$X_{k+1} = \begin{pmatrix} X_k & O_k \\ O_k & X_k \end{pmatrix} \text{ and } O_{k+1} = \begin{pmatrix} O_k & X_k \\ X_k & 4O_k \end{pmatrix},$$

for $k = 0, 1, \ldots, m-3$. Here $\|N\|$ denotes the sum of elements of matrix N.

Oh and colleagues refer to these matrices X_k and O_k as *state matrices*. The authors utilize this state matrix recursion to bound the growth rate of knot mosaics [6, 8, 1], and Oh further adapts the method to solve problems in monomer and dimer tilings [5, 7]. An unexamined direction in this research program is modifying the suitably connected property. This motivates us to introduce *messy polygon mosaics* using the tiles set $\mathbb{T}$ from [2], and enumerate them with state matrices as in [9].

2 Messy Polygon Mosaics

Definition 2.1. A *messy polygon mosaic* is a mosaic that contains at least one polygon.

Figure 4 shows two examples of messy polygon $(5,7)$ mosaics, both of which contain 3 polygons. In both examples, we shade the tiles that make up each polygon in gray.

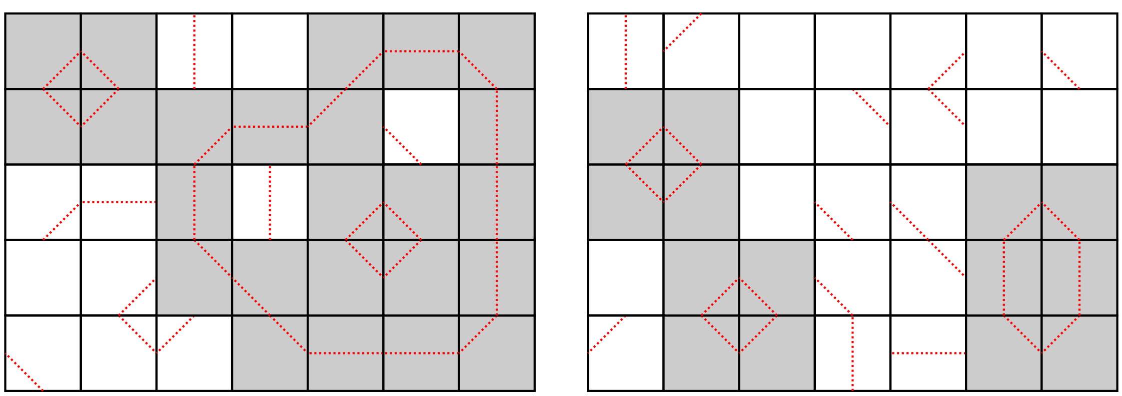

Figure 4: Messy polygon mosaics

The main goal of this paper is to enumerate messy polygon mosaics, but it turns out to be simpler to enumerate the number of mosaics that *do not* contain a polygon. Therefore, let $\mathbb{S}^{(m,n)}$ be the subset of (m,n) mosaics that do not contain a polygon. Clearly the number of messy polygon (m,n) mosaics is then $7^{mn} - \left|\mathbb{S}^{(m,n)}\right|$.

From the fact that the smallest polygon is made of 4 tiles, shown in Figure 5, we can conclude that $\left|\mathbb{S}^{(n,1)}\right| = 7^n$, and $\left|\mathbb{S}^{(2,2)}\right| = 7^4 - 1$. For $n, m \geq 2$, we first define the state matrices for messy polygon mosaics.

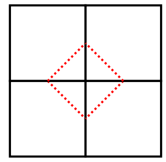

Figure 5: The smallest polygon

Definition 2.2. For integers $k \geq 1$ let A_k, B_k, C_k, D_k be $2^{k-1} \times 2^{k-1}$ matrices with integer entries, where $A_1 = \begin{pmatrix} 7 \end{pmatrix}, B_1 = \begin{pmatrix} -1 \end{pmatrix}, C_1 = \begin{pmatrix} 1 \end{pmatrix}, D_1 = \begin{pmatrix} 1 \end{pmatrix}$ and

$$A_{k+1} = \begin{pmatrix} 7A_k & B_k \\ C_k & D_k \end{pmatrix} \quad B_{k+1} = \begin{pmatrix} -A_k & B_k \\ 0C_k & D_k \end{pmatrix}$$
$$C_{k+1} = \begin{pmatrix} A_k & 0B_k \\ C_k & D_k \end{pmatrix} \quad D_{k+1} = \begin{pmatrix} A_k & -B_k \\ C_k & 7D_k \end{pmatrix}.$$

Our main result is Theorem 2.1.

Theorem 2.1. *The number of* (m, n) *mosaics that do not contain a polygon* $\left|\mathbb{S}^{(m,n)}\right|$ *is the* $(0, 0)$ *entry of* A_n^m.

3 Preliminaries

We begin by defining a mapping f between a mosaic in $\mathbb{M}^{(m,n)}$ to an (m, n) *binary lattice*. An (m, n) binary lattice is a rectangular lattice of $m + 1$ by $n + 1$ vertices, with each vertex labeled 0 or 1. We also define a *framed* binary lattice to be a binary lattice in which the boundary vertices are labeled 0. An example of a $(5, 7)$ framed binary lattice is shown on the right of Figure 6. Also let $\mathbb{L}^{(m,n)}$ be the set of all (m, n) binary lattices and $\mathbb{F}^{(m,n)}$ be the set of all (m, n) framed binary lattices. We immediately have $\left|\mathbb{L}^{(m,n)}\right| = 2^{(m+1)(n+1)}$, $\left|\mathbb{F}^{(m,n)}\right| = 2^{(m-1)(n-1)}$.

Definition 3.1. $f : \mathbb{M}^{(m,n)} \to \mathbb{F}^{(m,n)}$ takes a mosaic and labels each vertex with the following rule. If the vertex is surrounded by an even number of polygons (including 0 polygons), label it 0. If the vertex is surrounded by an odd number of polygons, label it 1. Removing the red dotted lines from the tiles gives the framed binary lattice.

Notice that by the definition of f, in a binary lattice polygons draw out the boundary between edge-connected vertices with the same label, excluding the vertices that are edge-connected to the boundary 0's. For example in Figure 6 the three polygons correspond with the boundary of the three edge-connected regions of vertices that are not edge-connected to the boundary 0's.

To enumerate $|\mathbb{S}^{(m,n)}|$, it will be useful to consider how f maps individual tiles in $\mathbb{T}$ to individual *cells* in a binary lattice.

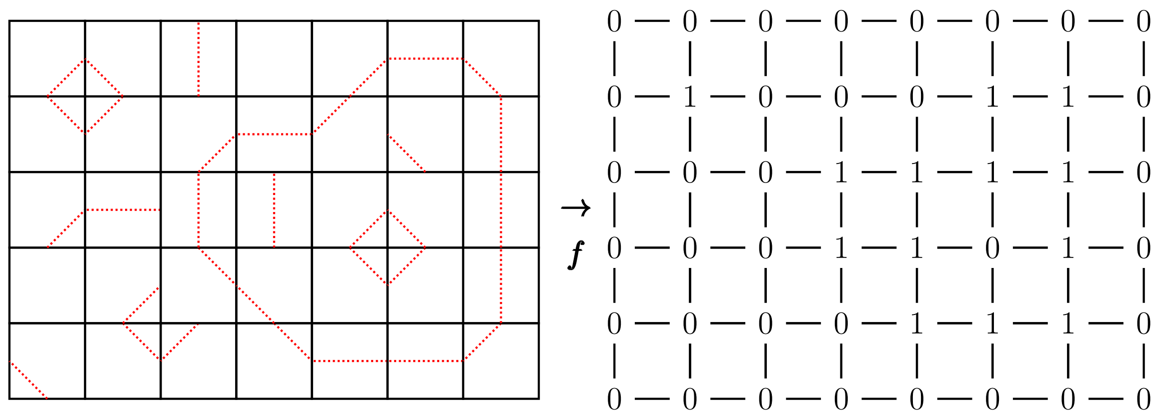

Figure 6: f applied to the left mosaic in Figure 4, resulting in a binary lattice

Definition 3.2. Let a *cell* be a $(1,1)$ binary lattice.

Example 3.1. Applying f to the mosaic in Figure 6 results in the top-left tile T_2 mapping to the top-left cell diagrammed below.

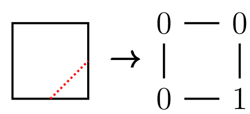

For convenience, we denote a cell by the 2×2 matrix of its vertex labels. For example, we denote the cell in Example 3.1 as $\begin{smallmatrix}0&0\\0&1\end{smallmatrix}$. The set of all unique cells is

$$\left\{\begin{smallmatrix}0&0\\0&0\end{smallmatrix}, \begin{smallmatrix}0&0\\0&1\end{smallmatrix}, \begin{smallmatrix}0&0\\1&0\end{smallmatrix}, \begin{smallmatrix}0&0\\1&1\end{smallmatrix}, \begin{smallmatrix}0&1\\0&0\end{smallmatrix}, \begin{smallmatrix}0&1\\0&1\end{smallmatrix}, \begin{smallmatrix}0&1\\1&0\end{smallmatrix}, \begin{smallmatrix}0&1\\1&1\end{smallmatrix}, \begin{smallmatrix}1&0\\0&0\end{smallmatrix}, \begin{smallmatrix}1&0\\0&1\end{smallmatrix}, \begin{smallmatrix}1&0\\1&0\end{smallmatrix}, \begin{smallmatrix}1&0\\1&1\end{smallmatrix}, \begin{smallmatrix}1&1\\0&0\end{smallmatrix}, \begin{smallmatrix}1&1\\0&1\end{smallmatrix}, \begin{smallmatrix}1&1\\1&0\end{smallmatrix}, \begin{smallmatrix}1&1\\1&1\end{smallmatrix}\right\}.$$

Definition 3.3. For a given (m,n), let ℓ^* be the framed binary lattice made of only $\begin{smallmatrix}0&0\\0&0\end{smallmatrix}$ cells.

Therefore, as all mosaics that do not contain a polygon map to ℓ^* under f, we have

$$\mathbb{S}^{(m,n)} = f^{-1}(\{\ell^*\}), \tag{1}$$

and so it suffices to compute $|f^{-1}(\{\ell^*\})|$.

It would be convenient to compute $f^{-1}(\ell)$ for any binary lattice ℓ "cell-by-cell". Let $u : \mathbb{L}^{(m,n)} \to \mathbb{Z}$ map a binary lattice ℓ to the product over all cells in ℓ with each term being

$$\begin{cases} 7 & \text{for cells } \begin{smallmatrix}0&0\\0&0\end{smallmatrix}, \begin{smallmatrix}1&1\\1&1\end{smallmatrix} \\ 0 & \text{for cells } \begin{smallmatrix}0&1\\1&0\end{smallmatrix}, \begin{smallmatrix}1&0\\0&1\end{smallmatrix} \\ 1 & \text{otherwise,} \end{cases}$$

where these terms come from the number of tiles that can map to a specific cell under f. However, as $|f^{-1}(\begin{smallmatrix}0&0\\0&0\end{smallmatrix})| = 7$, for the (m,n) binary lattice ℓ^*, we would get

$$u(\ell^*) = 7^{mn} = |\mathbb{M}^{(m,n)}| > |\mathbb{S}^{(m,n)}|.$$

Clearly, this approach overcounts $|\mathbb{S}^{(m,n)}|$. We can examine this phenomena more closely by first definining g.

Definition 3.4. $g : \mathbb{F}^{(m,n)} \to \mathbb{M}^{(m,n)}$ takes a framed binary lattice that does not contain the cells $\begin{smallmatrix}0&1\\1&0\end{smallmatrix}$ or $\begin{smallmatrix}1&0\\0&1\end{smallmatrix}$, and constructs a mosaic by replacing all $\begin{smallmatrix}0&0\\0&0\end{smallmatrix}$ and $\begin{smallmatrix}1&1\\1&1\end{smallmatrix}$ cells with T_0, and replacing all other cells with the unique tile that maps to that cell under f.

Notice that for some binary lattice ℓ, $g(\ell)$ is not necessarily equal to $f^{-1}(\ell)$, as g only returns polygon mosaics and not messy polygon mosaics. We can now examine the overcounting more closely.

Example 3.2. Consider the following binary lattices and mosaics for $(m,n) = (4,2)$.

$$\begin{array}{ccccc} 0 & - & 0 & - & 0 \\ | & & | & & | \\ 0 & - & 1 & - & 0 \\ | & & | & & | \\ 0 & - & 0 & - & 0 \\ | & & | & & | \\ 0 & - & 0 & - & 0 \\ | & & | & & | \\ 0 & - & 0 & - & 0 \end{array} \qquad \begin{array}{ccccc} 0 & - & 0 & - & 0 \\ | & & | & & | \\ 0 & - & 0 & - & 0 \\ | & & | & & | \\ 0 & - & 0 & - & 0 \\ | & & | & & | \\ 0 & - & 1 & - & 0 \\ | & & | & & | \\ 0 & - & 0 & - & 0 \end{array} \qquad \begin{array}{ccccc} 0 & - & 0 & - & 0 \\ | & & | & & | \\ 0 & - & 1 & - & 0 \\ | & & | & & | \\ 0 & - & 0 & - & 0 \\ | & & | & & | \\ 0 & - & 1 & - & 0 \\ | & & | & & | \\ 0 & - & 0 & - & 0 \end{array}$$

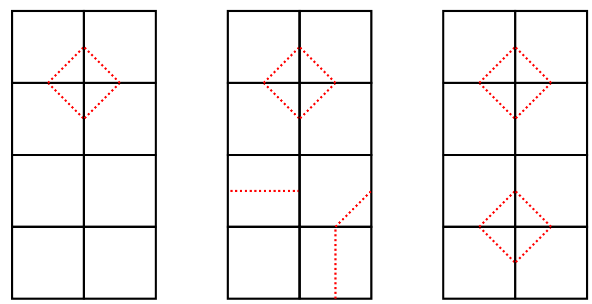

ℓ_1 ℓ_2 ℓ_3 Mosaic 1 Mosaic 2 Mosaic 3

We have $u(\ell_1) = 7^4, u(\ell_2) = 7^4$, and $u(\ell_3) = 1$. We also have $f(\text{Mosaic } 3) = \ell_3$. Each cell in the bottom two rows of ℓ_1 map to 7 possible tiles. However, 1 of the 7^4 permutations forms a new polygon in these bottom two rows. This is also true for the top two rows of ℓ_2. Therefore, $u(\ell_1)$, $u(\ell_2)$, and $u(\ell_3)$ all count Mosaic 3.

Surprisingly, this overcounting phenomena can be remedied by a small modificiation to u, which we call v.

Definition 3.5. Let $v : \mathbb{L}^{(m,n)} \to \mathbb{Z}$ map a binary lattice ℓ to the product over all cells in ℓ with each term being

$$\begin{cases} 7 & \text{for cells } \begin{smallmatrix}0&0\\0&0\end{smallmatrix}, \begin{smallmatrix}1&1\\1&1\end{smallmatrix} \\ 0 & \text{for cells } \begin{smallmatrix}0&1\\1&0\end{smallmatrix}, \begin{smallmatrix}1&0\\0&1\end{smallmatrix} \\ -1 & \text{for cells } \begin{smallmatrix}0&0\\1&0\end{smallmatrix}, \begin{smallmatrix}1&0\\1&1\end{smallmatrix} \\ 1 & \text{otherwise} \end{cases}$$

and the empty product being 1.

Example 3.3. If we let ℓ be the framed binary lattice on the right of Figure 6, we have $v(\ell) = -7^{11}$.

We will first show that $v(\ell)$, which is computed "cell-by-cell" from ℓ, recovers global information about the number of polygons in $g(\ell)$ if ℓ is framed.

Definition 3.6. For a framed binary lattice ℓ, let $p(\ell)$ to be the number of polygons in the polygon mosaic $g(\ell)$.

Proposition 3.1. *If ℓ is a framed binary lattice that does not contain the cells $\begin{smallmatrix}0&1\\1&0\end{smallmatrix}$ or $\begin{smallmatrix}1&0\\0&1\end{smallmatrix}$, then*

$$sign(v(\ell)) = (-1)^{p(\ell)}. \tag{2}$$

Proof. For this proof, we use LHS and RHS to abbreviate the left and right hand side of Equation 2. We prove the result by induction. For the base case, construct the $(1, n)$ framed binary lattice ℓ for some $n \geq 1$. As there are no cells in ℓ, from the definition of v the LHS is $v(\ell) = 1$. As there no polygons in $g(\ell)$, we have the RHS is 1.

For the induction step, fix an (m, n) framed binary strip ℓ for $m \geq 1$. Then consider an $(m+1, n)$ framed binary strip ℓ' that shares the top $m-1$ rows of vertices with ℓ and an arbitrarily-labelled m-th row, such that there are no $\begin{smallmatrix}0&1\\1&0\end{smallmatrix}$ or $\begin{smallmatrix}1&0\\0&1\end{smallmatrix}$ cells. We show that we can construct ℓ' from ℓ with a procedure that preserves Equation 2 with each intermediate step.

Procedure:

Step a. Add a bottom row to ℓ of $n+1$ vertices all labeled 0. This results in a new $(m+1, n)$ framed binary lattice we denote ℓ_a.

Step b. Scanning rows $m-1$ and m of ℓ' left to right, if there exists a column of the form $\begin{smallmatrix}1\\1\end{smallmatrix}$, change the associated $\begin{smallmatrix}1\\0\end{smallmatrix}$ column in ℓ_a to $\begin{smallmatrix}1\\1\end{smallmatrix}$. Completing this scan results in a new framed binary lattice denoted ℓ_b.

Step c. Scanning rows $m-1$ and m of ℓ' left to right, if there exists a column of the form $\begin{smallmatrix}0\\1\end{smallmatrix}$, change the associated $\begin{smallmatrix}0\\0\end{smallmatrix}$ column in ℓ_b to $\begin{smallmatrix}0\\1\end{smallmatrix}$. Completing this scan results in the framed binary lattice ℓ'.

For step a, only $\begin{smallmatrix}0&0\\0&0\end{smallmatrix}$ cells are added. As $\text{sign}\left(v\left(\begin{smallmatrix}0&0\\0&0\end{smallmatrix}\right)\right) = 1$, the LHS is unchanged. For the RHS, no new edge-connected regions are created, no new polygons are created in $g(\ell_a)$ so Equation 2 is preserved by step a.

For steps b and c, we encounter two distinct cases which we diagram in Figure 7. These diagrams have $a, b, c, d \in [0, 1]$, and use the # symbol to indicate the vertex being changed from a 0 to a 1.

$$\begin{array}{ccccc} \mathrm{a} & — & 1 & — & \mathrm{b} \\ | & & | & & | \\ \mathrm{c} & — & \# & — & 0 \\ | & & | & & | \\ 0 & — & 0 & — & 0 \end{array}$$

(a) Step b. Diagram

$$\begin{array}{ccccc} \mathrm{a} & — & 0 & — & \mathrm{b} \\ | & & | & & | \\ \mathrm{c} & — & \# & — & \mathrm{d} \\ | & & | & & | \\ 0 & — & 0 & — & 0 \end{array}$$

(b) Step c. Diagram

Figure 7: Step Diagrams

For step b, Figure 7a depicts all possible cases one can encounter scanning left to right on ℓ_a. Note that the vertex right of the # symbol must be 0, as the procedure moving left to right on ℓ_a gives that this vertex must be 0.

Notice that no assignment of a, b, and c can create cells $\begin{smallmatrix}0&0\\1&0\end{smallmatrix}$ or $\begin{smallmatrix}1&0\\1&1\end{smallmatrix}$. Additionally, it cannot be the case that $a = 0$ and $c = 1$, as that would imply that ℓ' contains the cell $\begin{smallmatrix}0&1\\1&0\end{smallmatrix}$. Therefore we have $\text{sign}(v(\ell_b)) = \text{sign}(v(\ell_a))$, so the LHS is preserved. Also note that because a polygon in $g(\ell)$ is an edge-connected set of vertices with the same label (not including the boundary 0's), that for all assignments of a, b, c, step b only involves one edge-connected set of vertices. Therefore, we have $p(\ell_a) = p(\ell_b)$, and so the RHS is preserved.

For step c, Figure 7b depicts all possible cases one can encounter scanning left to right on ℓ_b. It cannot be the case that $a = 1$ and $c = 0$, as this would imply ℓ' contains $\begin{smallmatrix}1&0\\0&1\end{smallmatrix}$. Similarly, it cannot be the cases that $b = 1$ and $d = 0$, as this would imply ℓ_b contains $\begin{smallmatrix}0&1\\1&0\end{smallmatrix}$. Additionally, it cannot be the case that $b = 0$ and $d = 1$, as the procedure moves left-to-right. This results in the following 6 cases, which we show each preserve Equation 2.

$$\begin{array}{ccccc} 0 & - & 0 & - & 0\\ | & & | & & | \\ 0 & - & \# & - & 0 \\ | & & | & & |\\ 0 & - & 0 & - & 0\end{array}$$

(a)

$$\begin{array}{ccccc} 0 & - & 0 & - & 1\\ | & & | & & | \\ 0 & - & \# & - & 1 \\ | & & | & & |\\ 0 & - & 0 & - & 0\end{array}$$

(b)

$$\begin{array}{ccccc} 0 & - & 0 & - & 0\\ | & & | & & | \\ 1 & - & \# & - & 0 \\ | & & | & & |\\ 0 & - & 0 & - & 0\end{array}$$

(c)

$$\begin{array}{ccccc} 0 & - & 0 & - & 1\\ | & & | & & | \\ 1 & - & \# & - & 1 \\ | & & | & & |\\ 0 & - & 0 & - & 0\end{array}$$

(d)

$$\begin{array}{ccccc} 1 & - & 0 & - & 0\\ | & & | & & | \\ 1 & - & \# & - & 0 \\ | & & | & & |\\ 0 & - & 0 & - & 0\end{array}$$

(e)

$$\begin{array}{ccccc} 1 & - & 0 & - & 1\\ | & & | & & | \\ 1 & - & \# & - & 1 \\ | & & | & & |\\ 0 & - & 0 & - & 0\end{array}$$

(f)

Figure 8: Step c. Cases

In Case 8a, the flip add one $\begin{smallmatrix}0&0\\1&0\end{smallmatrix}$ cell, so the sign of the LHS changes. As the flip creates a new edge-connected region, a new polygon is created, and so the sign of the RHS changes.

In Case 8b, the flip does not add a $\begin{smallmatrix}0&0\\1&0\end{smallmatrix}$ cell or $\begin{smallmatrix}1&0\\1&1\end{smallmatrix}$ cell, so the sign of the LHS stays the same. As the flip does not create a new edge-connected region, the RHS stays the same.

In Case 8c, the flip removes and adds a $\begin{smallmatrix}0&0\\1&0\end{smallmatrix}$ cell, so the sign of the LHS stays the same. As the flip does not create a new edge-connected region, the RHS stays the same.

In Case 8d, the flip removes a $\begin{smallmatrix}0&0\\1&0\end{smallmatrix}$ cell, so the sign of the LHS changes. Before the flip, either the two edge-connected regions of 1's are distinct in the full framed binary lattice, or they are joined. After the flip, if the regions were distinct, they are now joined, and so 1 polygon is removed. If the regions were joined, a new edge-connected region of 0's (that is not connected to the boundary) is created, and so 1 polygon is created. Either way, the RHS changes.

In Case 8e, the flip adds both a $\begin{smallmatrix}0&0\\1&0\end{smallmatrix}$ cell and a $\begin{smallmatrix}1&0\\1&1\end{smallmatrix}$ cell, so the sign of the LHS stays the same. As the flip does not create a new edge-connected region, the RHS stays the same.

In Case 8f, the flip adds $\begin{smallmatrix}1&0\\1&1\end{smallmatrix}$, so the sign of the LHS changes. The same logic from Case 8d applies, as the flip either removes or adds a polygon, so the RHS changes.

As all cases preserve Equation 2, the $(m+1,n)$ framed binary lattice ℓ' also follows Equation 2. $\square$

We point out here that the function v if defined for all binary lattices, while Proposition 3.1 only holds for framed binary lattices that do not contain cells $\begin{smallmatrix}0&1\\1&0\end{smallmatrix}$ or $\begin{smallmatrix}1&0\\0&1\end{smallmatrix}$.

Proposition 3.2. *The number of* (m,n) *mosaics that do not contain a polygon has*

$$\sum_{\ell \in \mathbb{F}^{(m,n)}} v(\ell) = \left|\mathbb{S}^{(m,n)}\right|.$$

Proof. TODO $\square$

As in Theorem 1.2 from [9], we can compute $\sum_{\ell \in \mathbb{F}^{(m,n)}} v(\ell)$ efficiently using the state matrix recursion method.

Definition 3.7. Let A_k, B_k, C_k, D_k be $2^{k-1} \times 2^{k-1}$ matrices with integer entries, where $A_1 = v(\begin{smallmatrix}0&0\\0&0\end{smallmatrix}), B_1 = v(\begin{smallmatrix}0&0\\1&0\end{smallmatrix}), C_1 = v(\begin{smallmatrix}1&0\\0&0\end{smallmatrix}), D_1 = v(\begin{smallmatrix}1&0\\1&0\end{smallmatrix})$, and for integers $k > 1$,

$$A_{k+1} = \begin{pmatrix} v(\begin{smallmatrix}0&0\\0&0\end{smallmatrix})A_k & v(\begin{smallmatrix}0&0\\0&1\end{smallmatrix})B_k \\ v(\begin{smallmatrix}0&1\\0&0\end{smallmatrix})C_k & v(\begin{smallmatrix}0&1\\0&1\end{smallmatrix})D_k \end{pmatrix} \quad B_{k+1} = \begin{pmatrix} v(\begin{smallmatrix}0&0\\1&0\end{smallmatrix})A_k & v(\begin{smallmatrix}0&0\\1&1\end{smallmatrix})B_k \\ v(\begin{smallmatrix}0&1\\1&0\end{smallmatrix})C_k & v(\begin{smallmatrix}0&1\\1&1\end{smallmatrix})D_k \end{pmatrix}$$
$$C_{k+1} = \begin{pmatrix} v(\begin{smallmatrix}1&0\\0&0\end{smallmatrix})A_k & v(\begin{smallmatrix}1&0\\0&1\end{smallmatrix})B_k \\ v(\begin{smallmatrix}1&1\\0&0\end{smallmatrix})C_k & v(\begin{smallmatrix}1&1\\0&1\end{smallmatrix})D_k \end{pmatrix} \quad D_{k+1} = \begin{pmatrix} v(\begin{smallmatrix}1&0\\1&0\end{smallmatrix})A_k & v(\begin{smallmatrix}1&0\\1&1\end{smallmatrix})B_k \\ v(\begin{smallmatrix}1&1\\1&0\end{smallmatrix})C_k & v(\begin{smallmatrix}1&1\\1&1\end{smallmatrix})D_k \end{pmatrix}.$$

Proposition 3.3. *The number of* (m,n) *mosaics that do not contain a polygon is the* $(0,0)$ *entry of* A_n^m*.*

Proof. TODO $\square$

Let the k digit binary representation of the number n be written as $\beta_k(n)$

TODO new end?

Intuitively, we would hope that for a binary lattice ℓ, $U(\ell)$ would equal $|f^{-1}(\{\ell\})|$. However this is not necessarily the case, as $U(\ell)$ does not *just* count the number of mosaics that map to ℓ under f.

Example 3.4. We have $U(\ell^*) = 7^{mn} = |\mathbb{M}^{(m,n)}|$, which clearly overcounts $|\mathbb{S}^{(m,n)}|$.

Examples 3.4 and 3.2 show we cannot compute $|f^{-1}(\{\ell\})|$ for a given binary lattice ℓ using $U(\ell)$, as cells $(00,00)$ and $(11,11)$ lead to over counting mosaics. Instead, U counts the number of mosaics that map to some set of binary lattices under f. This set is defined in Definition 3.11. To define this set, we first point out that a binary lattice can be split into the cells that have $u_{(i,j)} = 7$ and the cells that have $u_{(i,j)} = 1$.

Definition 3.8. A polygon $\mathcal{P}$ is *specified* by a binary lattice ℓ if the cells in ℓ that map to the tiles that make up $\mathcal{P}$ all have $u_{(i,j)} = 1$.

Definition 3.9. Let $P : \mathbb{L}^{(m,n)} \to \mathbb{N}$ be the number of polygons specified in a binary lattice ℓ.

Example 3.5. From Example 3.2, ℓ_1 specifies the polygon in the top 2 rows of Mosaic 2, as the cells in the top 2 rows of ℓ_1 all have $u_{(i,j)} = 1$. However ℓ_1 does not specify the polygon in the bottom 2 rows of Mosaic 2, as the cells in the bottom 2 rows of ℓ_1 all have $u_{(i,j)} = 7$. ℓ_3 specifies both polygons in Mosaic 2. Therefore $P(\ell_1) = P(\ell_2) = 1$, and $P(\ell_3) = 2$.

Example 3.6. The binary lattice ℓ^* specifies 0 polygons, and so $P(\ell^*) = 0$.

Definition 3.10. For binary lattices ℓ, ℓ', we say $\ell \leq \ell'$ if one can construct ℓ' by flipping the parity of some number of vertices (possibly 0 vertices) in ℓ, such that all polygons specified by ℓ are unchanged and no cells with index $(01, 10)$ or $(10, 01)$ are created.

Definition 3.11. For a binary lattice ℓ, let $\mathbb{U}(\ell) = \{\ell' | \ell \leq \ell'\}$.

Example 3.7. From Example 3.2, $\ell_1 \leq \ell_3$ as one can construct ℓ_3 from ℓ_1 by flipping the vertex at $(3, 1)$ from 0 to 1. As ℓ_1 specifies the polygon in the top two rows of Mosaic 2, and this vertex flip does not change the top polygon, $\ell_1 \leq \ell_3$. We also have $\ell_1 \leq \ell_1$ simply by selecting no vertices to flip. As diagrammed below, constructing ℓ_4 from ℓ_1 by flipping the vertex at $(2, 1)$ does change a polygon specified by ℓ_1, and so $\ell_1 \not\leq \ell_4$.

$$\begin{array}{ccccc} 0 & — & 0 & — & 0 \\ | & & | & & | \\ 0 & — & 1 & — & 0 \\ | & & | & & | \\ 0 & — & 1 & — & 0 \\ | & & | & & | \\ 0 & — & 0 & — & 0 \\ | & & | & & | \\ 0 & — & 0 & — & 0 \end{array}$$

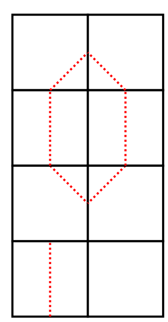

ℓ_4 Mosaic 3

Therefore $\mathbb{U}(\ell_1) = \{\ell_1, \ell_3\}$, $\mathbb{U}(\ell_2) = \{\ell_2, \ell_3\}$, and $\mathbb{U}(\ell_3) = \{\ell_3\}$.

Example 3.8. Every binary lattice ℓ has $\ell^* \leq \ell$, as ℓ^* specifies 0 polygons. Therefore for a given (m, n), we have $\mathbb{U}(\ell^*) = \mathbb{L}^{(m,n)}$.

Proposition 3.4. *For all ℓ we have*

$$U(\ell) = \sum_{\ell' \in \mathbb{U}(\ell)} |f^{-1}(\{\ell'\})|. \tag{3}$$

Proof. For a binary lattice $\ell' \in \mathbb{U}(\ell)$, ℓ' specifies new polygons without changing any of the polygons specified in ℓ. Consider the set of cells S that differ between ℓ and ℓ'. By definition, these cells in ℓ all have $u_{(i,j)} = 7 = |\mathbb{T}|$, while in ℓ' they all have $u_{(i,j)} = 1$. Also by definition $U(\ell)$ enumerates every possible combination of tiles that could map to each cell in S. Therefore, the tiles sthat specify the new polygons in ℓ' are counted, and so $|f^{-1}(\ell')|$ is also counted by U. □

Surprisingly, we can recover $|\mathbb{S}^{(m,n)}|$ by first considering how much each mosaic is over-counted in

$$\sum_{\ell \in \mathbb{L}^{(m,n)}} U(\ell). \tag{4}$$

Proposition 3.5.

$$\sum_{\ell \in \mathbb{L}^{(m,n)}} U(\ell) = \sum_{\ell \in \mathbb{L}^{(m,n)}} \sum_{\ell' \in \mathbb{U}(\ell)} |f^{-1}(\{\ell'\})| = \sum_{\ell \in \mathbb{L}^{(m,n)}} \left(\sum_{p=0}^{P(\ell)} \binom{P(\ell)}{p} \right) |f^{-1}(\{\ell\})|. \tag{5}$$

Proof. The first equality follows directly from Proposition 3.4. For the second equality, for a given binary lattice ℓ the coefficient of $|f^{-1}(\{\ell\})|$ is the number of elements in $\{\ell' | \ell' \leq \ell\}$. Therefore, a binary lattice is in $\{\ell' | \ell' \leq \ell\}$ if the binary lattice only specifies $0 \leq p \leq P(\ell)$ of the $P(\ell)$ polygons specified by ℓ. As there are $\binom{P(\ell)}{p}$ ways to specify p polygons from a choice of $P(\ell)$ polygons, this gives the second equality for all $P(\ell) > 0$.

If ℓ' has $P(\ell') = 0$, then $\ell' = \ell^*$. As $\{\ell' | \ell' \leq \ell^*\} = \{\ell^*\}$, the term $|f^{-1}(\ell')|$ is only counted once. As $1 = \binom{0}{0}$, this completes the proof. □

Proposition 3.6. *The number of (m,n) mosaics that do not contain a polygon $|\mathbb{S}^{(m,n)}|$ has*

$$|\mathbb{S}^{(m,n)}| = \sum_{\ell \in \mathbb{L}^{(m,n)}} (-1)^{P(\ell)} U(\ell). \tag{6}$$

Proof. If we group terms like the second equality of Equation 5, we get

$$\sum_{\ell \in \mathbb{L}^{(m,n)}} (-1)^{P(\ell)} U(\ell) = \sum_{\ell \in \mathbb{L}^{(m,n)}} \left(\sum_{p=0}^{P(\ell)} (-1)^{P(\ell)} \binom{P(\ell)}{p} \right) |f^{-1}(\{\ell\})|.$$

By the binomial theorem, for $P(\ell) > 0$ we have

$$\sum_{p=0}^{P(\ell)} (-1)^{P(\ell)} \binom{P(\ell)}{p} = (1-1)^{P(\ell)} = 0,$$

so all terms where $P(\ell) > 0$ are 0. As the only binary lattice with $P(\ell) = 0$ is ℓ^*, we have

$$\sum_{\ell \in \mathbb{L}^{(m,n)}} (-1)^{P(\ell)} U(\ell) = \binom{0}{0} |f^{-1}(\ell^*)| = |\mathbb{S}^{(m,n)}|.$$

□

4 A Cell-Level Identity

Though Equation 6 does compute $|\mathbb{S}^{(m,n)}|$, computing the number of polygons specified in a binary lattice $P(\ell)$ requires examining the entire structure of ℓ. It will be more efficient to recover the $(-1)^{P(\ell)}$ term at the level of individual cells. More concretely, we seek a function V of the form

$$V(\ell) := \prod_{\text{Cell } (i,j) \in \ell} v_{(i,j)},$$

such that for all ℓ

$$(-1)^{P(\ell)} U(\ell) = V(\ell). \tag{7}$$

The idea is to add a coefficient $p_{(i,j)} \in \{-1, 1\}$ to each value of $u_{(i,j)}$ in such a way as to recover the $(-1)^{P(\ell)}$ term. With this in mind we define $v_{(i,j)} := p_{(i,j)} u_{(i,j)}$.

Condition 4.1. *A subset of cells $\mathcal{S}$ in a binary lattice ℓ meets this condition if*

$$\prod_{\textit{Cell } (i,j) \in \mathcal{S}} p_{(i,j)} = -1, \tag{8}$$

with $p_{(i,j)} \in \{-1, 1\}$.

Cells in a binary lattice either do or do not specify a polygon. To recover the $(-1)^{P(\ell)}$ term, the following must be true. Cells that cannot specify a polygon must all have $p_{(i,j)} = 1$. Moreover, if a set of cells specifies any one polygon, it must meet Condition 4.1.

Proposition 4.2. *There exists values $p_{(i,j)}$ for which the cells that do not specify a polygon have $p_{(i,j)} = 1$, and Condition 4.1 holds for any set of cells that specify a polygon.*

Proof. We can immediately see $p_{(00,00)} = p_{(11,11)} = p_{(01,10)} = p_{(10,01)} = 1$, as cells $(00, 00)$, $(11, 11)$, $(01, 10)$, and $(10, 01)$ can never be in the subset of cells that specify a polygon, and so must be positive.

For the remaining values of $p_{(i,j)}$, we first examine the cells that map to the smallest polygon, shown in Figure 5.

$$\begin{array}{ccccc} 0 & — & 0 & — & 0 \\ | & & | & & | \\ 0 & — & 1 & — & 0 \\ | & & | & & | \\ 0 & — & 0 & — & 0 \end{array} \qquad\qquad \begin{array}{ccccc} 1 & — & 1 & — & 1 \\ | & & | & & | \\ 1 & — & 0 & — & 1 \\ | & & | & & | \\ 1 & — & 1 & — & 1 \end{array}$$

Figure 9: Portions of binary lattices associated with the smallest polygon

For the portions of binary lattices in Figure 9, Condition 4.1 amounts to the following two equations

$$
\begin{aligned}
p_{(00,01)}p_{(00,10)}p_{(01,00)}p_{(10,00)} &= -1 \\
p_{(11,10)}p_{(11,01)}p_{(10,11)}p_{(01,11)} &= -1.
\end{aligned} \tag{9}
$$

We refer to the equations above as *constraints*, as they constrain the possible assignments of $p_{(i,j)}$.

To define the remaining constraints, consider the unbounded square lattice with all vertices labeled 0, except for the origin labeled 1. We refer to this as the *starting position*.

From the definition of f we know that polygons are the boundary of edge-connected vertices of the same label. Clearly one can construct arbitrary sets of edge-connected 0's and 1's from the starting position by flipping the parity of a vertex one-by-one.

This *bit flip* operation, depicted in Figure 10, corresponds with changing the identity of the four cells that share that vertex. As each cell has its associated $p_{(i,j)}$ value, it must be the case that the bit flip preserves Condition 4.1 for the cells involved. Additionally, as the surrounding 8 vertices are unchanged udner this operation, we must define 2^8 constraints.

In each of the constraints, the parity of the number of edge-connected regions of 1s must either change or stay the same after the bit flip. If the parity remains unchanged, the bit flip is of *Type 1*, and if the parity changes the bit flip is of *Type 2*.

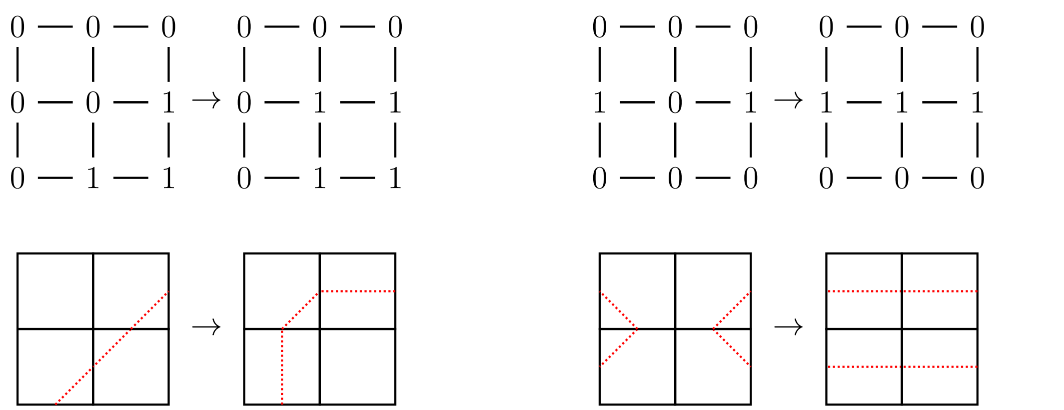

(a) Type 1 bit flip and associated tiles

(b) Type 2 bit flip and associated tiles

Figure 10: Bit flips for binary lattices

For a bit flip of *Type 1*, to adhere to Condition 4.1, the associated constraint is that the sign of the product of the related cells must stay the same after the flip. For example, Figure 10a represents the constraint

$$
p_{(01,00)}p_{(11,01)}p_{(00,00)}p_{(01,00)} = p_{(01,01)}p_{(11,11)}p_{(01,00)}p_{(11,00)}. \tag{10}
$$

For a bit flip of *Type 2*, to adhere to Condition 4.1, the associated constraint is that the sign of the product of the related cells must change after the flip. For example, Figure 10b represents the constraint

$$
p_{(00,10)}p_{(00,01)}p_{(10,00)}p_{(01,00)} = -p_{(00,11)}p_{(00,11)}p_{(11,00)}p_{(11,00)}. \tag{11}
$$

In Figure 10b the transformation corresponds with *either* two distinct polygons joining into one polygon *or* one polygon splitting into two distinct polygons. In either case, we want the sign of the product to change to adhere to Condition 4.1.

This gives a procedure to define the 2^8 bit flip constraints on $p_{(i,j)}$. Before solving for $p_{(i,j)}$, we can discard any constraint that involves cells $(01, 10)$ or $(10, 01)$, as we don't consider any binary lattices with these cells.

Finally, we can then use software to verify that all remaining constraints admit a solution.

□

We summarize the values of $p_{(i,j)}$ and $v_{(i,j)}$ in Table 1.

Cell (i, j)	$\mathbf{u_{(i,j)}}$	$\mathbf{p_{(i,j)}}$	$\mathbf{v_{(i,j)}}$	**Cell (i, j)**	$\mathbf{u_{(i,j)}}$	$\mathbf{p_{(i,j)}}$	$\mathbf{v_{(i,j)}}$
$(00, 00)$	7	1	7	$(11, 11)$	7	1	7
$(00, 01)$	1	1	1	$(11, 10)$	1	-1	-1
$(00, 10)$	1	1	1	$(11, 01)$	1	1	1
$(00, 11)$	1	1	1	$(11, 00)$	1	1	1
$(01, 00)$	1	1	1	$(10, 11)$	1	1	1
$(01, 01)$	1	1	1	$(10, 10)$	1	1	1
$(01, 10)$	0	1	0	$(10, 01)$	0	1	0
$(01, 11)$	1	1	1	$(10, 00)$	1	-1	-1

Table 1: Values of $p_{(i,j)}$ and $v_{(i,j)}$

We can then write

$$\sum_{\ell \in \mathbb{L}^{(m,n)}} V(\ell) = |\mathbb{S}^{(m,n)}|. \tag{12}$$

Following other work with mosaics, $|\mathbb{S}^{(m,n)}|$ can be calculated more efficiently than in Equation 12 using the state matrix recursion introduced in [9].

5 Proof of Theorem 2.1

This argument is an adaptation of the proof in [9] for binary lattices.

Let a *binary sub-lattice* of size (p, q) be a rectangular lattice of $p+1$ by $q+1$ vertices, in which only the left and right boundary vertices must be labeled 0, and all other vertices can be labeled 0 or 1. Also let $\hat{\mathbb{L}}^{(p,q)}$ be the set of all binary sub-lattices of size (p, q). We choose a similar indexing convention for binary sub-lattices as individual cells, in which we, ignoring the first and last 0, read the bottom row and the top row as two binary numbers (i, j) respectively. For example, Figure 11 is a binary sub-lattice of size $(2, 4)$ with index $(011, 100)$.

Note that for $p > 1$, this index does not uniquely define the binary sub-lattice.

As with binary lattices, we can compute $V(\hat{\ell})$ for a binary sub-lattice $\hat{\ell} \in \hat{\mathbb{L}}^{(p,q)}$. We can now define the *state matrix* for $\hat{\mathbb{L}}^{(p,q)}$ to be the $2^q \times 2^q$ matrix $A^{(p,q)} = (A^{(p,q)}_{i,j})$ where element

$$
\begin{array}{ccccccccc}
0 & — & 1 & — & 0 & — & 0 & — & 0 \\
| & & | & & | & & | & & | \\
0 & — & 0 & — & 1 & — & 0 & — & 0 \\
| & & | & & | & & | & & | \\
0 & — & 0 & — & 1 & — & 1 & — & 0
\end{array}
$$

Figure 11: A binary sub-lattice of size $(2,4)$ with index $(011,100)$

$$A^{(p,q)}_{i,j} = \sum_{\hat{\ell} \text{ with index } (i,j)} V(\hat{\ell}).$$

Here $A_{i,j}$ is the entry in the i-th row of the matrix, read top-to-bottom, and in the j-th column of the matrix read left-to-right. As the binary sub-lattices $\hat{\mathbb{L}}^{(p,q)}$ with index $(0\dots0, 0\dots0)$ are just the binary lattices $\mathbb{L}^{(p,q)}$, we have for a state matrix $A^{(p,q)}$ that

$$A^{(p,q)}_{0,0} = \sum_{\ell \in \mathbb{L}^{(p,q)}} V(\ell).$$

Theorem 2.1 amounts to an efficient procedure to compute $A^{(p,q)}$.

Proposition 5.1. *For the set $\hat{\mathbb{L}}^{(1,q)}$ the associated state matrix $A^{(1,q)}$ can be computed by first defining $A^{(1,2)} = \begin{bmatrix} 7^2 & -1 \\ 1 & 1 \end{bmatrix}$. We recursively define $A^{(1,q)} \in \mathbb{Z}^{2^q \times 2^q}$ given $A^{(1,q-1)}$. Begin by writing $A^{(1,k)} = \begin{bmatrix} A_{[0,0]} & A_{[0,1]} \\ A_{[1,0]} & A_{[1,1]} \end{bmatrix}$, where the block matrices $A_{[i,j]}$ are square block matrices of size $2^{k-1} \times 2^{k-1}$. We then have*

$$A^{(1,k+1)} = \begin{bmatrix} 7A_{[0,0]} & 7A_{[0,1]} & 7^{-1}A_{[0,0]} & A_{[0,1]} \\ 7A_{[1,0]} & 7A_{[1,1]} & 0A_{[1,0]} & A_{[1,1]} \\ -7^{-1}A_{[0,0]} & 0A_{[0,1]} & 7^{-1}A_{[0,0]} & A_{[0,1]} \\ A_{[1,0]} & A_{[1,1]} & -A_{[1,0]} & 7A_{[1,1]} \end{bmatrix}.$$

Proof. We use induction on q. We can immediately calculate the entries of $A^{(1,2)}$ by listing all size $(1,2)$ binary sub-lattices, then using the definition of V.

$$
\begin{array}{ccccc}
0 & — & 0 & — & 0 \\
| & & | & & | \\
0 & — & 0 & — & 0
\end{array}
\qquad
\begin{array}{ccccc}
0 & — & 1 & — & 0 \\
| & & | & & | \\
0 & — & 0 & — & 0
\end{array}
$$

$$
\begin{array}{ccccc}
0 & — & 0 & — & 0 \\
| & & | & & | \\
0 & — & 1 & — & 0
\end{array}
\qquad
\begin{array}{ccccc}
0 & — & 1 & — & 0 \\
| & & | & & | \\
0 & — & 1 & — & 0
\end{array}
$$

Above gives

$$\begin{bmatrix} v_{(00,00)}v_{(00,00)} & v_{(00,01)}v_{(00,10)} \\ v_{(01,00)}v_{(10,00)} & v_{(01,01)}v_{(10,10)} \end{bmatrix} = \begin{bmatrix} 7^2 & -1 \\ 1 & 1 \end{bmatrix}.$$

We then assume that the statement for $A^{(1,k)}$ is true up to k. Within $A^{(1,k)}$, consider all the size $(1,k)$ binary sub-lattices counted in the entries of the upper left $2^{k-1} \times 2^{k-1}$ block matrix, which we denote $A_{[0,0]}$. By construction, all of these binary sub-lattices have indexes of the form $(0\ldots,0\ldots)$, in which both indexes begin with a 0. Similarly, the upper right $2^{k-1} \times 2^{k-1}$ block matrix $A_{[0,1]}$ counts all binary sub-lattices with indexes like $(0,\ldots,1\ldots)$, and so on.

To construct binary sub-lattices of size $(1,k+1)$, we then append one of each of the four cells in Figure 12 to the left of every size $(1,k)$ binary sub-lattices, such that the former left boundary 0's are replaced.

$$\begin{array}{ccc} 0 - 0 & \quad & 0 - 1 \\ | \quad\; | & & | \quad\; | \\ 0 - 0 & & 0 - 0 \\ \textbf{(00, 00)} & & \textbf{(00, 01)} \\[1em] 0 - 0 & & 0 - 1 \\ | \quad\; | & & | \quad\; | \\ 0 - 1 & & 0 - 1 \\ \textbf{(01, 00)} & & \textbf{(01, 01)} \end{array}$$

Figure 12: Appending cells

An example of appending cell $(01,00)$ to the size $(1,3)$ binary sub-lattice $(11,10)$ is shown below.

$$\begin{array}{c} 0 - 0 \\ | \quad\; | \\ 0 - 1 \end{array} + \begin{array}{c} 0 - 1 - 0 - 0 \\ | \quad\; | \quad\; | \quad\; | \\ 0 - 1 - 1 - 0 \end{array} \to \begin{array}{c} 0 - 0 - 1 - 0 - 0 \\ | \quad\; | \quad\; | \quad\; | \quad\; | \\ 0 - 1 - 1 - 1 - 0 \end{array}$$

This creates the size $(1,4)$ binary sub-lattice $(111,010)$. Notice this operation only changes the identity of the two left-most cells, namely changing the left-most $(01,01)$ cell into cells $(01,00)$ and $(11,01)$.

By construction, as every binary sub-lattice counted in the block matrix $A_{[1,1]}$ has an index of the form $(1\ldots,1\ldots)$, the entries in $A_{[1,1]}$ are all divisible by $v_{01,01}$. Therefore, the size $(1,k+1)$ binary sub-lattices with index of the form $(11\ldots,01\ldots)$ are counted by $(v_{01,00}v_{11,01}/v_{01,01})A_{[1,1]}$.

Performing the appending operation with each of the four cells from Figure 12 to each other gives 16 possible pairs, which we diagram below such that it is consistent with the indexing for $A^{(1,k)}$.

$$\begin{array}{ccccc} 0 & - & 0 & - & 0 \\ | & & | & & | \\ 0 & - & 0 & - & 0 \end{array} \qquad \begin{array}{ccccc} 0 & - & 0 & - & 1 \\ | & & | & & | \\ 0 & - & 0 & - & 0 \end{array} \qquad \begin{array}{ccccc} 0 & - & 1 & - & 0 \\ | & & | & & | \\ 0 & - & 0 & - & 0 \end{array} \qquad \begin{array}{ccccc} 0 & - & 1 & - & 1 \\ | & & | & & | \\ 0 & - & 0 & - & 0 \end{array}$$

$$\begin{array}{ccccc} 0 & - & 0 & - & 0 \\ | & & | & & | \\ 0 & - & 0 & - & 1 \end{array} \qquad \begin{array}{ccccc} 0 & - & 0 & - & 1 \\ | & & | & & | \\ 0 & - & 0 & - & 1 \end{array} \qquad \begin{array}{ccccc} 0 & - & 1 & - & 0 \\ | & & | & & | \\ 0 & - & 0 & - & 1 \end{array} \qquad \begin{array}{ccccc} 0 & - & 1 & - & 1 \\ | & & | & & | \\ 0 & - & 0 & - & 1 \end{array}$$

$$\begin{array}{ccccc} 0 & - & 0 & - & 0 \\ | & & | & & | \\ 0 & - & 1 & - & 0 \end{array} \qquad \begin{array}{ccccc} 0 & - & 0 & - & 1 \\ | & & | & & | \\ 0 & - & 1 & - & 0 \end{array} \qquad \begin{array}{ccccc} 0 & - & 1 & - & 0 \\ | & & | & & | \\ 0 & - & 1 & - & 0 \end{array} \qquad \begin{array}{ccccc} 0 & - & 1 & - & 1 \\ | & & | & & | \\ 0 & - & 1 & - & 0 \end{array}$$

$$\begin{array}{ccccc} 0 & - & 0 & - & 0 \\ | & & | & & | \\ 0 & - & 1 & - & 1 \end{array} \qquad \begin{array}{ccccc} 0 & - & 0 & - & 1 \\ | & & | & & | \\ 0 & - & 1 & - & 1 \end{array} \qquad \begin{array}{ccccc} 0 & - & 1 & - & 0 \\ | & & | & & | \\ 0 & - & 1 & - & 1 \end{array} \qquad \begin{array}{ccccc} 0 & - & 1 & - & 1 \\ | & & | & & | \\ 0 & - & 1 & - & 1 \end{array}$$

The associated appending equations for the $v_{i,j}$ values are then

$$\begin{array}{llll}
\dfrac{v_{(00,00)}v_{(00,00)}}{v_{(00,00)}} = 7 & \dfrac{v_{(00,00)}v_{(00,01)}}{v_{(00,01)}} = 7 & \dfrac{v_{(00,01)}v_{(00,10)}}{v_{(00,00)}} = 7^{-1} & \dfrac{v_{(00,01)}v_{(00,11)}}{v_{(00,01)}} = 1 \\
\dfrac{v_{(00,00)}v_{(01,00)}}{v_{(01,00)}} = 7 & \dfrac{v_{(00,00)}v_{(01,01)}}{v_{(01,01)}} = 7 & \dfrac{v_{(00,01)}v_{(01,10)}}{v_{(01,00)}} = 0 & \dfrac{v_{(00,01)}v_{(01,11)}}{v_{(01,01)}} = 1 \\
\dfrac{v_{(01,00)}v_{(10,00)}}{v_{(00,00)}} = -7^{-1} & \dfrac{v_{(01,00)}v_{(10,01)}}{v_{(00,01)}} = 0 & \dfrac{v_{(01,01)}v_{(10,10)}}{v_{(00,00)}} = 7^{-1} & \dfrac{v_{(01,01)}v_{(10,11)}}{v_{(00,01)}} = 1 \\
\dfrac{v_{(01,00)}v_{(11,00)}}{v_{(01,00)}} = 1 & \dfrac{v_{(01,00)}v_{(11,01)}}{v_{(01,01)}} = 1 & \dfrac{v_{(01,01)}v_{(11,10)}}{v_{(01,00)}} = -1 & \dfrac{v_{(01,01)}v_{(11,11)}}{v_{(01,01)}} = 7
\end{array}$$

We can then determine

$$A^{(1,k+1)} = \begin{bmatrix} 7A_{[0,0]} & 7A_{[0,1]} & 7^{-1}A_{[0,0]} & A_{[0,1]} \\ 7A_{[1,0]} & 7A_{[1,1]} & 0A_{[1,0]} & A_{[1,1]} \\ -7^{-1}A_{[0,0]} & 0A_{[0,1]} & 7^{-1}A_{[0,0]} & A_{[0,1]} \\ A_{[1,0]} & A_{[1,1]} & -A_{[1,0]} & 7A_{[1,1]} \end{bmatrix}.$$

□

Proposition 5.2. *For the set $\mathbb{L}^{(p,q)}$, the state matrix has*

$$A^{(p,q)} = (A^{(1,q)})^p.$$

Proof. We use induction on p, and assume $A^{(k,q)} = (A^{(1,q)})^k$. Therefore,

$$A^{(k,q)}_{i,j} = \sum_{\hat{\ell} \text{ with index } (i,j)} V(\hat{\ell})$$

for $\hat{\ell}$ of size (k,q) and index (i,j). Notice that we can build all binary sub-lattices of size $(k+1,q)$ with index (i,j) by the following. Append a size $(1,q)$ binary sub-lattice of index

(i, s) and a size (k, q) binary sub-lattice of index (s, j). For example, Figure 13 adjoins a size $(2, 3)$ binary sub-lattice with index $(10, 01)$ to a size $(1, 3)$ binary sub-lattice with index $(01, 11)$.

$$\begin{array}{ccccccc}
0 & - & 1 & - & 1 & - & 0 \\
| & & | & & | & & | \\
0 & - & 0 & - & 1 & - & 0 \\
 & & & + & & & \\
0 & - & 0 & - & 1 & - & 0 \\
| & & | & & | & & | \\
0 & - & 0 & - & 0 & - & 0 \\
| & & | & & | & & | \\
0 & - & 1 & - & 0 & - & 0
\end{array}
\quad \to \quad
\begin{array}{ccccccc}
0 & - & 1 & - & 1 & - & 0 \\
| & & | & & | & & | \\
0 & - & 0 & - & 1 & - & 0 \\
| & & | & & | & & | \\
0 & - & 0 & - & 0 & - & 0 \\
| & & | & & | & & | \\
0 & - & 1 & - & 0 & - & 0
\end{array}$$

Figure 13: Appending a size $(1, 3)$ binary sub-lattice to a size $(2, 3)$ sub-lattice

Doing this append operation for all s amounts to

$$A_{i,j}^{(k+1,q)} = \sum_{s=0}^{2^q-1} A_{i,s}^{(k,q)} A_{s,j}^{(1,q)},$$

which gives

$$A^{(k+1,q)} = A^{(k,q)} A^{(1,q)} = (A^{(1,q)})^{k+1}.$$

□

6 Acknowledgements

The authors would like to thank Michael Maltenfort for the edits, improvements and ideas for this paper.

References

[1] Dooho Choi et al. "Quantum knot mosaics and bounds of the growth constant". In: *Reviews in Mathematical Physics* 36.10 (2024), p. 2450025. DOI: 10.1142/S0129055X24500259. eprint: https://doi.org/10.1142/S0129055X24500259. URL: https://doi.org/10.1142/S0129055X24500259.

[2] Kyungpyo Hong and Seungsang Oh. "Bounds on Multiple Self-avoiding Polygons". In: *Canadian Mathematical Bulletin* 61.3 (Sept. 2018), pp. 518–530. ISSN: 1496-4287. DOI: 10.4153/cmb-2017-072-x. URL: http://dx.doi.org/10.4153/CMB-2017-072-x.

[3] Samuel J. Lomonaco and Louis H. Kauffman. "Quantum knots and mosaics". In: *Quantum Information Processing* 7.2 (2008), pp. 85–115. DOI: 10.1007/s11128-008-0076-7. URL: https://doi.org/10.1007/s11128-008-0076-7.

[4] OEIS Foundation Inc. *The On-Line Encyclopedia of Integer Sequences*. Published electronically at `http://oeis.org`.

[5] Seungsang Oh. "Domino tilings of the expanded Aztec diamond". In: *DISCRETE MATHEMATICS* 341.4 (Apr. 2018), pp. 1185–1191. ISSN: 0012-365X. DOI: `10.1016/j.disc.2017.10.016`.

[6] Seungsang Oh. "Quantum knot mosaics and the growth constant". In: *Topology and its Applications* 210 (2016), pp. 311–316. ISSN: 0166-8641. DOI: `https://doi.org/10.1016/j.topol.2016.08.011`. URL: `https://www.sciencedirect.com/science/article/pii/S0166864116301857`.

[7] Seungsang Oh. "State matrix recursion method and monomer-dimer problem". In: *DISCRETE MATHEMATICS* 342.5 (May 2019), pp. 1434–1445. ISSN: 0012-365X. DOI: `10.1016/j.disc.2019.01.022`.

[8] Seungsang Oh and Youngin Kim. "Growth rate of quantum knot mosaics". In: *Quantum Information Processing* 18.8 (2019), p. 238. DOI: `10.1007/s11128-019-2353-z`. URL: `https://doi.org/10.1007/s11128-019-2353-z`.

[9] Seungsang Oh et al. "Quantum knots and the number of knot mosaics". In: *Quantum Information Processing* 14.3 (2015), pp. 801–811. DOI: `10.1007/s11128-014-0895-7`. URL: `https://doi.org/10.1007/s11128-014-0895-7`.